The onset of nonpenetrative convection in a suddenly cooled layer of fluid

Christian F. Ihle [a], Yarko Niño [b,*]

[a] *Program in Fluid Dynamics, Facultad de Ciencias Físicas y Matemáticas, Universidad de Chile, Blanco Encalada 2002 Of. 327, Santiago, Chile*
[b] *Departamento de Ingenieria Civil, Division de Recursos Hidricos y Medio Ambiente, Universidad de Chile, Av. Blanco Encalada 2002, Santiago, Chile*

Abstract

Conditions for the onset of nonpenetrative convection in a horizontal Boussinesq fluid layer subject to a step change in temperature are studied using propagation theory. A wide range of Prandtl numbers and two different kinematic boundary conditions are considered. It is shown that for high Rayleigh numbers, critical conditions for the onset of convective motion reproduce exactly those for the unsteady Rayleigh–Bénard instability. Present results extend those of previous research and show a tendency of the rigid–rigid and free–rigid critical curves to converge for low Prandtl numbers. Comparison between present and previously reported results on critical conditions for the onset of instabilities and onset time using different methods yields good agreement on a middle to high Prandtl number range. A ratio of 10 between experimentally measured and theoretically predicted onset times is suggested for stress-free bounded systems.

Keywords: Buoyancy-driven instability; Critical time; Nonpenetrative convection; Prandtl number; Propagation theory; Rayleigh number; Isothermal heating

1. Introduction

Nonpenetrative convection is defined by Adrian [1] as the unstable flow field that derives from the existence of a fluid layer heated from below (or cooled from above) with adiabatic top (or bottom if cooled from above), resembling Bénard convection [2]. This thermal boundary condition precludes the existence of a steady flow regime. Nonpenetrative convection represents a reasonable assumption in a variety of physical problems, that range from ventilation and air conditioning (like, for instance, cold storage rooms and warehouses with poor insulation from one side) to earth sciences, particularly regarding the dynamics of the planetary boundary layer [3]. In this paper, the attention is focused on the study of conditions for the onset of impulsively generated nonpenetrative convection. Here, the base state of the system to be perturbed, at difference from the one that gives rise to Bénard convection [4], is unsteady due to the existence of a thermally diffusive state whose temporal rate of change is high at the very beginning of the evolution. Hence, a stability model able to deal with this difficulty is to be considered.

After early approaches to the analysis of the stability of unsteady systems (e.g. 'frozen time' and 'quasi-static' models, reviewed by Gresho and Sani [5] and Homsy [6], respectively), the study of the onset of manifest convection in high Rayleigh number fluid layers impulsively heated or cooled began with Foster [7], who used an initial value technique, so-called 'amplification model', which considers a transient evolution of the base state. In this case, disturbances that cause the onset of convection are assumed to occur only initially. The major drawback of this method is that determination of amplification requires the knowledge of amplitudes of initial disturbances, for all the

* Corresponding author. Tel.: +562 6968448; fax: +562 6894171.
E-mail address: ynino@ing.uchile.cl (Y. Niño).

Nomenclature

a_s, b_s	coefficients of Eqs. (10) and (11), respectively, $s = 1, \ldots, 5$ (integer), or ∞
(a_x, a_y)	dimensionless horizontal wavevector
a	dimensionless horizontal wavenumber, $\sqrt{a_x^2 + a_y^2}$
C	concentration [kmol/m^3] or designation of constant value
C_p	specific heat of the fluid at constant pressure [J kg^{-1} K^{-1}]
D	mass diffusion coefficient [m^2/s]
$\mathrm{D}(\cdot)$	ordinary derivative with respect to ζ, $\mathrm{d}(\cdot)/\mathrm{d}\zeta$
$\partial_{\chi(\psi)}(\cdot)$	partial derivative, $\partial(\cdot)/\partial\chi$ or $\partial^2(\cdot)/\partial\chi\psi$
DP	deep pool acronym
g	gravity vector (pointing in the direction of z axis) [m s^{-2}]
k	thermal conductivity of the fluid [W m^{-1} K^{-1}]
L	depth of the fluid layer [m]
Pr	Prandtl number, $v\alpha^{-1}$
r	slope of the geometrical sequence to extrapolate critical Ra_τ values
t	time (dimensionless if no superscript)
u	velocity, (u, v, w) (dimensional or not depending on the superscript. w is ζ-dependent if no superscript is present)
Ra	Rayleigh number, $g\beta(\theta^*_{\max} - \theta^*_{\min})L^3 v^{-1}\alpha^{-1}$
Ra_τ	τ-dependent Rayleigh number, $\tau^{3/2}Ra$
TBL	thermal boundary layer acronym
(x, y, z)	Cartesian coordinates (dimensionless if no superscript is present)

Greek symbols

α	thermal diffusivity of the fluid [m^2 s^{-1}]
β	thermal expansion coefficient [K^{-1}]
λ	relative difference coefficient, $\max_\zeta\{100 \times \lvert 1 - \theta_0/\theta_{0\mathrm{DP}}\rvert\}$
δ_θ	dimensionless thermal penetration depth
Δ	Laplacian operator (dimensional or not depending on the superscript)
Δ_1	horizontal Laplacian operator (dimensional or not depending on the superscript)
γ	concentration coefficient of expansion [kg/kmol]
ζ	self-similar vertical coordinate, $z/\sqrt{t}$
θ	temperature (self-similar if no superscript, otherwise dimensional or dimensionless)
v	kinematic viscosity of the fluid [m^2 s^{-1}]
σ	temporal growth rate for disturbances
τ	definition for time in the self-similar framework, $\tau = t$

Subscripts

0	base state
1	disturbance, or correlative assignment to constant
2–5	correlative assignment to constant
b	bulk
c	critical state
DP	deep pool assumption: ζ-only dependence
linear	linear boundary forcing
∞	infinite Prandtl number
m	experimental detection
min	minimal condition
max	maximal condition
u	thermal advection dominance over pure diffusivity
step	step boundary forcing
τ	τ-dependent variable: $\Gamma_\tau \equiv \tau^\phi \Gamma$

Superscripts

*	dimensional length, temperature, time, velocity or differential operator
$\sim$	dimensionless temperature, velocity or differential operator
–	root-mean-square

wavelengths present on the eigenfunction expansion. As this is impossible, Foster's approach consisted of a heuristic procedure that combined the assumption of several disturbance patterns along with experimental observations [8]. Using a different approach, Jhaveri and Homsy [9] and Kim and Kim [10] used random forcing functions to solve an initial value problem to find the onset times, both for step and ramp-heated systems of high Rayleigh numbers, suggesting a definition of the onset time as that corresponding to a certain excess of the computed Nusselt number with respect to the purely conductive one.

More recently, Kim et al. [11] studied the impulsively driven Rayleigh–Bénard problem with initial stratification, using the method called by these authors 'propagation theory' [12–14]. Its basis lies on the assumption that most of the disturbances are confined within the thermal penetration depth, which is considered as a length scale, leading to the transformation of the linearized equations into self-similar forms. In more recent contributions, Chung et al. [15] and Choi et al. [16] suggest new definitions for onset times, taking into account nonlinear effects that come from the numerical simulation of the unsteady Rayleigh–Bénard problem and compare them with results obtained using propagation theory. In the latter work, the influence of initial stratification on the distribution of the mentioned time scales is analyzed.

In an experimental context, Spangenberg and Rowland [17] studied the onset of evaporative convection using Schlieren photography techniques, while Foster [18], by means of radiometry, showed that surface temperature in suddenly cooled evaporative systems evolves in a linear fashion. Plevan and Quinn [19], Blair and Quinn [20] and later Tan and Thorpe [21], measured onset times in nonevaporative systems whose stability depends on the concentration of gases into water. Their results, in the context of the present research, are commented in Section 4. Goldstein and Volino [22], studied the onset of convection on a thick fluid layer heated impulsively from below. Their work presents also an extensive review of literature focused on the transient features of natural convection.

In this paper, propagation theory was the chosen stability method to assess the onset of nonpenetrative convective motion. For high thermal perturbations, it is shown that this phenomenon behaves the same as the onset of unsteady Rayleigh–Bénard convection. This result allows for a side by side comparison of present computations with numerical and experimental results reported in the context of the latter problem. Some new findings in that regard are presented and discussed as well.

2. Problem description

An initially quiescent horizontal fluid layer, well mixed at temperature $\theta^* = \theta^*_{\max}$, infinite on its horizontal dimension but finite, with height L, on the vertical axis z^*, is suddenly cooled, by dropping its surface temperature, at time $t^* = 0$ and $z^* = 0$, to $\theta^* = \theta^*_{\min}$. Surface is to be kept at this lower temperature for $t^* > 0$ (Fig. 1).

For high enough temperature step: $\delta\theta^* = \theta^*_{\max} - \theta^*_{\min}$, a buoyancy-driven circulation is induced. This problem can be modeled using continuity, Navier–Stokes and energy equations on a Boussinesq fluid, with no heat sources present. Surface tension effects in the free–rigid case are neglected in the present study. This assumption is reasonable in the present context, as shown experimentally by Davenport and King [23] in the case of linearly heated deep reservoirs. Scales to be used are L to form dimensionless coordinates (x, y, and z), $L^2\alpha^{-1}$ to form dimensionless time, t, αL^{-1} to form dimensionless velocity base state and perturbations, $(\tilde{u}_0, \tilde{v}_0, \tilde{w}_0)$ and $(\tilde{u}_1, \tilde{v}_1, \tilde{w}_1)$, respectively. $v\alpha g^{-1}\beta^{-1}L^{-3}$, to form dimensionless temperature perturbation, $\tilde{\theta}_1$, whereas the dimensionless base temperature, $\tilde{\theta}_0$, is scaled to range between 0 and 1: $\tilde{\theta}_0 = (\theta^*_0 - \theta^*_{\min})(\theta^*_{\max} - \theta^*_{\min})^{-1}$. α, v and β are the thermal diffusivity, kinematic viscosity, and thermal expansion coefficient of the fluid, respectively. g is the magnitude of the gravity vector, which points in the same direction of the z axis. In the latter expressions, the subscript 0 refers to the base state and 1 to the perturbed one.

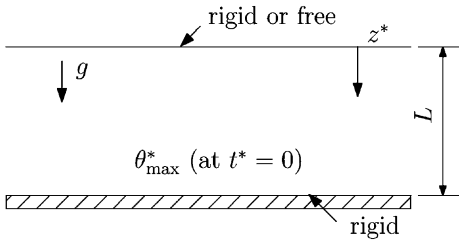

Fig. 1. Problem configuration. z^* axis points downward.

A first order expansion for the dimensionless temperature and velocity is considered, with the form $\tilde{\theta} = \tilde{\theta}_0 - \tilde{\theta}_1$, and $\tilde{\mathbf{u}} = \tilde{\mathbf{u}}_0 + \tilde{\mathbf{u}}_1 = \tilde{\mathbf{u}}_1 = (\tilde{u}_1, \tilde{v}_1, \tilde{w}_1)$, respectively. The minus sign on the expansion for temperature means that positive perturbations have a cooling effect. The base state is that of a horizontally infinite, quiescent fluid layer. Neglecting second order terms, the following set of equations is obtained for the vertical velocity and temperature perturbations:

$$\left(\frac{1}{Pr}\partial_t - \widetilde{\Delta}\right)\widetilde{\Delta}\tilde{w}_1 = \widetilde{\Delta}_1\tilde{\theta}_1, \tag{1a}$$

$$\partial_t\tilde{\theta}_1 - Ra\tilde{w}_1\partial_z\tilde{\theta}_0 = \widetilde{\Delta}\tilde{\theta}_1, \tag{1b}$$

where $Pr = v\alpha^{-1}$ corresponds to the Prandtl number and $Ra = g\beta(\theta^*_{\max} - \theta^*_{\min})L^3v^{-1}\alpha^{-1}$ corresponds to a Rayleigh number based on the overall temperature step, $\widetilde{\Delta} \equiv \partial_{xx} + \partial_{yy} + \partial_{zz}$ and $\widetilde{\Delta}_1 \equiv \widetilde{\Delta} - \partial_{zz}$, provided the dimensionless equation for the base state is satisfied:

$$\partial_t\tilde{\theta}_0 = \partial_{zz}\tilde{\theta}_0, \tag{2a}$$

$$\tilde{\theta}_0(t = 0, z) = 1, \quad \tilde{\theta}_0(t > 0, z = 0) = \partial_z\tilde{\theta}_0 \quad (t \geqslant 0, z = 1) = 0. \tag{2b}$$

The derivation of stability equations using propagation theory is analogous to that of Kang and Choi [14] and Yang and Choi [24]. Hence, only the essential steps are given here. In propagation theory it is stated that, for the case of thermal convection in systems where instabilities are confined mainly into the thermal boundary layer (TBL), a balance between viscous and buoyant forces can be made, such that it is possible to scale dimensionless vertical velocity perturbations with time as $|\tilde{w}_1\tilde{\theta}_1^{-1}| \sim \delta_\theta^2$, where $\delta_\theta \propto \sqrt{t}$ is the dimensionless thermal penetration depth. From the latter relation and dimensional analysis it can also be inferred that [24]:

$$[\tilde{\theta}_1(z,t), \tilde{w}_1(z,t)] = [t^n\theta_1(z/\sqrt{t}), t^{n+1}w_1(z/\sqrt{t})], \tag{3}$$

where n is a parameter. Now, stability equations are represented in a new coordinate system defined as $(t, \zeta = z/\sqrt{t})$, instead of (t, z), while $\tilde{\theta}_1$ and $\tilde{w}_1$ turn to θ_1 and w_1 in the newly defined system. To avoid confusion, t will be defined as τ. The present criterion for the setting of n is to find the lowest possible onset times from the characteristic problem. To this purpose, it must be set to zero [24]. Additionally, Choi et al. [16] and Chung et al. [15] argue that this condition can be also derived from the assumption that the onset time occurs when the growth rates of the root-mean-square values of the base state temperature and of the temperature perturbations are equal. In the context of a system with an imposed heat flux, the latter assumption leads to a different n value of 1/2 [25,26].

Eqs. (1) are cyclic in the horizontal plane. Then, modes with wavenumbers a_x and a_y for the x and y axis, respectively, are considered. Introducing (3) $\times \exp[\mathrm{i}(a_x x + a_y y)]$ in the latter system, noting that $\partial_\tau(\cdot) = -(2\tau)^{-1}\partial_\zeta(\cdot)$ and that $\partial_z(\cdot) = \tau^{-1/2}\partial_\zeta(\cdot)$, the set of stability equations to be solved is:

$$\left[(\mathrm{D}^2 - a_\tau^2)^2 + \frac{1}{2Pr}(\zeta \mathrm{D}^3 - a_\tau^2 \zeta \mathrm{D} + 2a_\tau^2)\right] w_1 - a_\tau^2 \theta_1 = 0, \tag{4a}$$

$$\left(\mathrm{D}^2 + \frac{1}{2}\zeta \mathrm{D} - a_\tau^2\right)\theta_1 + w_1 Ra_\tau \mathrm{D}\theta_0 = 0, \tag{4b}$$

where $\mathrm{D}^n(\cdot) = \mathrm{d}^n(\cdot)/\mathrm{d}\zeta^n$, $a_\tau = \tau^{1/2}\sqrt{a_x^2 + a_y^2}$ and $Ra_\tau = \tau^{3/2} Ra$.

The scaling assumed here, which considers the hypothesis that disturbances are confined mainly into a thermal penetration depth, makes Eqs. (4) valid for small values of time only. In this case, the base state for temperature, θ_0, can be expressed as a function exclusively of ζ. This kind of system, representative of a thermally semi-infinite one, is commonly named 'deep pool' system (the acronym DP will be adopted hereafter). Its TBL is small compared with the thickness of the fluid layer.

For large values of τ, when equations are not self-similar anymore, it has been shown [24,27] that eigenvalues for (4) can still be found. In those works, it was also shown that asymptotic convergence in time to results obtained with the frozen time model is achieved. However, the validity at intermediate values of time of the thermal scaling proposed here is not clear. Regarding this topic, an analysis on the validity of this model, in the context of nonpenetrative convection, is being presently prepared [28]. For the system with no-slip top and bottom surfaces (named herein as the rigid–rigid case), boundary conditions for the perturbed quantities are:

$$\theta_1 = w_1 = \mathrm{D}w_1 = 0 \quad \text{in } \zeta = 0, \tag{5a}$$

$$\mathrm{D}\theta_1 = w_1 = \mathrm{D}w_1 = 0 \quad \text{in } \zeta = 1/\sqrt{\tau}. \tag{5b}$$

In the case with stress-free top and no-slip bottom (defined also as the free–rigid case), boundary conditions which are to be applied to Eqs. (4) are:

$$\theta_1 = w_1 = \mathrm{D}^2 w_1 = 0 \quad \text{in } \zeta = 0, \tag{6a}$$

$$\mathrm{D}\theta_1 = w_1 = \mathrm{D}w_1 = 0 \quad \text{in } \zeta = 1/\sqrt{\tau}. \tag{6b}$$

The marginal stability problem to be considered is to solve: $\min_{a_\tau} Ra_\tau$, where a_τ and Ra_τ satisfy (4), with boundary conditions (5) or (6), in the rigid–rigid and free–rigid cases, respectively. This procedure is to be applied to the self-similar system, valid for small values of time. Under this condition, the present definition of the Rayleigh number is the same as the one used in the classical Rayleigh–Bénard problem, based on the temperature difference between the top and bottom horizontal boundaries, since here, the bottom boundary holds its higher temperature throughout the whole lapse of time during which the present stability model is valid.

3. Solution method

Eqs. (4) and the boundary conditions (5) and (6) are homogeneous. Then, the value of $\mathrm{D}^2 w_1(0)$ and $\mathrm{D}w_1(0)$ can be assigned arbitrarily in the rigid–rigid and free–rigid cases, respectively [14,27]. To solve the problem posed in the previous section, a solver based on the shooting method using a fourth order Runge–Kutta numerical integration formula was implemented. Convergence to minima was achieved using a Newton–Raphson scheme. Validation of the numerical implementation was done by analyzing the classical rigid–rigid Rayleigh–Bénard problem with a step change in the bottom temperature [11], using Eqs. (4). Monotonic, albeit slow convergence for increasing time, close to the well known value of the critical Rayleigh number of 1708 was found for different Prandtl numbers. This result numerically checks the classic result for the steady state problem, which states that the onset of the Rayleigh–Bénard instability does not depend on the Prandtl number [4]. This statement is recalled expressing (4) in the (z, t) space, re-scaling w_1 and θ_1 and their derivatives to $\tilde{w}_1$ and $\tilde{\theta}_1$ via (3), and taking the limit when $\tau \to \infty$. The resulting equations are $(\partial_{zz} - a^2)^2 \tilde{w}_1 = a^2 \tilde{\theta}_1$ and $(\partial_{zz} - a^2)\tilde{\theta}_1 + \tilde{w}_1 Ra = 0$, regardless of the value of Prandtl number, for which no assumption has been made but to be positive. Now, as the resulting expressions are only functions of z, it is noted that the latter equations also correspond to the linearized stability system obtained assuming an exponential growth rate, $\exp \sigma t$, with a critical stability condition $\sigma = 0$ [24]. This approach corresponds to the 'marginal state' variation of the frozen time model [5]. With this set of equations, the computed critical Rayleigh number and its associated wavenumber are 1707.7618 and 3.11632, respectively, in agreement with the pair (1707.765, 3.12) proposed by Sparrow et al. [29] and (1707.7618, 3.11635), computed by Mizushima [30].

In numerical terms, the DP system assumption means that the outer boundary to be considered goes to infinite. To reproduce this fact into the computation of eigenvalues prior to the minimization process, the extrapolation procedure described by Chen et al. [31] for critical Ra_τ numbers was used. Roughly, this approach is based on the observation that different Ra_{τ_n} numbers, obtained for different outer depths ζ_n, decrease approximately as a geometrical sequence. Then, the asymptotic Rayleigh number can be computed as $Ra_\tau^0 \approx Ra_{\tau_n}^0 + r(Ra_{\tau_n}^0 - Ra_{\tau_{n-1}}^0)/(1-r)$, where r is the slope of the approximately logarithmic line obtained using different pairs $(\zeta_n, Ra_{\tau n})$.

4. Results and discussion

4.1. Base state solutions

The base state solution can be calculated using Laplace transforms, which yields Eq. (7). This approach has the advantage of producing a series with faster convergence than that obtained through Fourier decomposition:

$$\theta_0(\zeta,\tau) = 1 + \sum_{n\geqslant 0}(-1)^{n+1}\left\{\operatorname{erfc}\left[\frac{n}{\sqrt{\tau}}+\frac{\zeta}{2}\right] + \operatorname{erfc}\left[\frac{n+1}{\sqrt{\tau}}-\frac{\zeta}{2}\right]\right\}. \quad (7)$$

The DP solution can be readily obtained solving (2) on a semi-infinite domain:

$$\theta_{0_{\mathrm{DP}}}(\zeta) = \operatorname{erfc}(\zeta/2). \quad (8)$$

For values of τ lower or close to 0.01 very small relative differences between Eqs. (7) and (8) are observed. Computing the latter as $\lambda = \max_\zeta\{100\times|1-\theta_0/\theta_{0\mathrm{DP}}|\}$, for $\tau = 0.005$, 0.007, 0.01, 0.02 and 0.05, $\lambda < 10^{-12}$, 10^{-12}, 10^{-10}, 10^{-4} and 0.1, respectively.

4.2. Comparison with the unsteady Rayleigh–Bénard problem

The deduction of the nonpenetrative stability problem in the light of the propagation model yields an interesting similitude with the unsteady Rayleigh–Bénard problem studied by Kim et al. [11]. Eqs. (4a) and (4b) have the same analytical expression than those corresponding to the latter work. The only difference between them is the thermal condition imposed at the boundary away from the step change in temperature (named herein as the outer boundary). In the present problem, the boundary condition $\lim_{\zeta\to\infty} \mathrm{D}\theta_1 = 0$ is imposed, while in Kim et al. [11], $\lim_{\zeta\to\infty}\theta_1 = 0$ is imposed instead, representing the existence of an isothermal outer boundary. It can be shown, however, that both types of outer boundary condition must be satisfied simultaneously in both problems. For fixed Rayleigh and Prandtl numbers, an onset time τ_c exists such that $\theta_1 = 0$ for $\tau < \tau_c = \tau_c(Pr, Ra)$ (i.e., the system does not experience convection before the onset time). On the other hand, the similarity condition inherent to the present propagation model imposes the scaling $\delta_\theta \sim \sqrt{\tau} \ll 1 (\tau \lll 1)$ for the thermal penetration depth, and the boundary condition $\mathrm{D}\theta_1(1/\sqrt{\tau}) = 0$. Then, considering, as stated previously, that the perturbations are mainly confined within the TBL, and assuming continuity of the temperature disturbance, necessarily $\theta_1(1/\sqrt{\tau}) = 0$, which is a mere consequence of the small penetration depth occurring at small times. As this holds for arbitrarily small onset times (and, consequently, arbitrarily large values of the Rayleigh number), if $\lim_{\zeta\to\infty}\mathrm{D}\theta_1 = 0$, then $\lim_{\zeta\to\infty}\theta_1 = 0$. Consequently, both problems, the impulsively isothermally heated Rayleigh–Bénard and the present nonpenetrative convection, are equivalent, provided the existence of a Rayleigh number range that support the deep-pool assumption.

Another interesting feature of the eigensystem (4) is that its eigenvalues are insensitive to the type of outer boundary condition considered, free or rigid, as can be verified with arguments similar to those of the previous paragraph. Hence, according to the propagation model, for high Rayleigh numbers the only boundary that matters to eigenvalues (both in the thermal and kinematic sense) is the one subjected to the impulsive change on temperature. This conclusion agrees with that of Foster [7], who noticed that motion was 'decoupled from the bottom', analyzing the problem of a surface-stress-free fluid layer subject to a step change in temperature, using the amplification model. Another consequence of this conclusion is that the free–rigid results to be presented here should be valid for the free–free and free–rigid variations of the Rayleigh–Bénard convection. The same applies, of course, to the free–free nonpenetrative convection problem, which offers a reasonable approximation to systems where a nearly stress-free, strong and stable density interface exists between two rather homogeneous layers of fluid. The latter, so-called 'thermocline' [32], is commonly found in lakes and reservoirs.

4.3. Solution of the eigenvalue problem

As $\tau \leqslant 0.01$ (which is bonded to the assumption of a highly supercritical system) must hold to keep the self-similarity of the base state, a lower bound to valid Rayleigh numbers is imposed

$$Ra(Pr) \geqslant Ra_{\min}(Pr) = \frac{Ra_\tau(Pr)}{0.01^{3/2}}. \quad (9)$$

Despite the existence of Kim et al. [11] results for the impulsively heated Rayleigh–Bénard problem, whose mathematical posing fully coincides with that of the present nonpenetrative convection problem as discussed in previous section, the eigenvalues for the rigid–rigid case were re-calculated here to serve as an additional validation of the numerical results obtained. Differences on computed values of Ra_τ were found only for $Pr = 100$, and even in that case they were not higher than about 1%. In the case of the a_τ computed values, a difference (of about 10%) was found for $Pr = 1$. The latter are indicative of an apparent error on Kim et al.'s [11] solution. Table 1 shows the minimum (a_τ, Ra_τ) eigenvalues computed for the DP system for a range of Prandtl numbers and the corresponding values of the minimum valid Rayleigh number, given by (9).

Results for the DP free–rigid case, which have not been previously reported in the context of the present problem and method, are shown in Fig. 2. The Ra_τ parameter varies exponentially for $Pr \leqslant 1$ and is virtually constant for values of $Pr > 1000$. The same trend occurs for the rigid–rigid case, as previously commented by Kim et al. [11,27]. Considering comments on Section 4.2, present data extend the results reported in the former work and are new to the nonpenetrative problem context. The following correlations, valid for $0.01 \leqslant Pr \leqslant 1000$, can be used to predict the onset time and the most unstable mode in the case of the DP system, for the free–rigid or rigid–rigid cases, with an error bound of 2%:

Table 1
Critical (a_τ, Ra_τ) parameters found for the DP system, as a function of Prandtl number

Pr	Rigid–rigid					Free–rigid		
	Present work		KCC99					
	a_τ	Ra_τ	a_τ	Ra_τ	$Ra_{\min}$	a_τ	Ra_τ	$Ra_{\min}$
0.01	0.824	1799.06	0.82	1799.1	1.80×10^6	0.809	1675.92	1.68×10^6
0.1	0.813	219.10	0.81	219.1	2.19×10^5	0.766	180.98	1.81×10^5
0.71	0.725	53.56	–	–	5.36×10^4	0.637	36.58	3.66×10^4
1	0.702	44.81	0.63	44.81	4.48×10^4	0.607	29.36	2.94×10^4
7	0.589	24.73	–	–	2.47×10^4	0.447	12.68	1.27×10^4
100	0.538	20.97	0.54	20.70	2.10×10^4	0.337	9.01	9.01×10^3
1000	0.533	20.70	0.53	20.69	2.07×10^4	0.320	8.67	8.67×10^3
∞	0.533	20.67	0.53	20.67	2.07×10^4	0.317	8.63	8.63×10^3

The fourth and fifth columns (labelled as KCC99) show the critical numbers found for the transient Rayleigh–Bénard problem studied by Kim et al. [11]. Columns 6 and 9 show the minimum Rayleigh numbers that guarantee that the DP assumption is valid both for the rigid–rigid and for the free–rigid system, respectively.

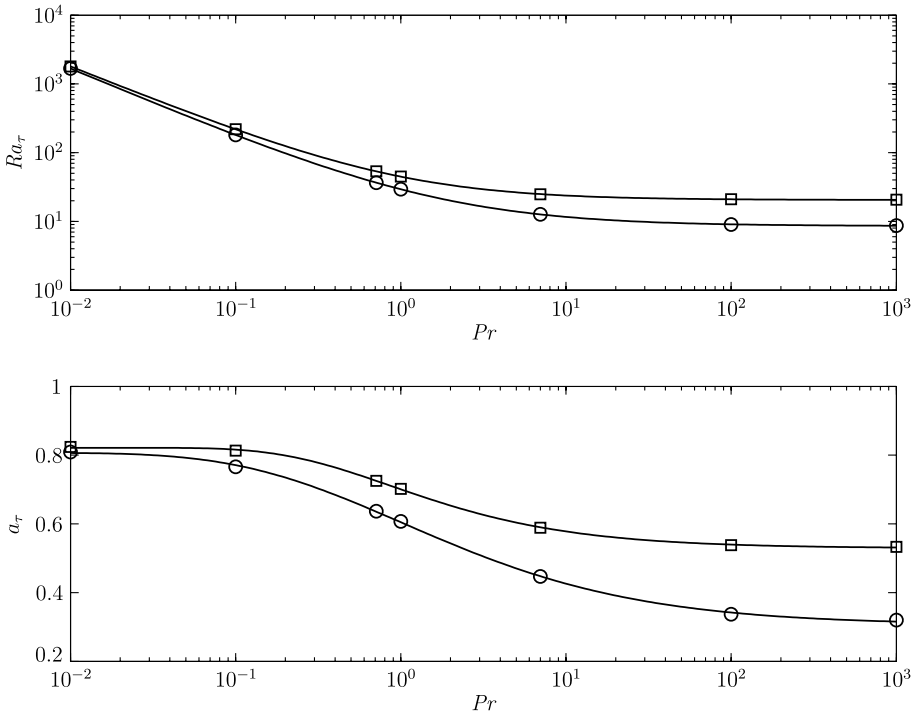

Fig. 2. Upper panel: effect of the Prandtl number on Ra_τ for the rigid–rigid and rigid–free cases. Lower panel: effect of the Prandtl number on the wavenumber of the fastest growing horizontal mode, a_c. Symbols represent calculated points, corresponding to Table 1: squares for the rigid–rigid case and circles for the free–rigid case. Curves represent interpolated results using the models given by Eqs. (10), and (11) and parameter sets given by Table 2.

$$\tau_c = a_1\left[a_2 + \left(\frac{a_3}{Pr}\right)^{a_4}\right]^{a_5} Ra^{-2/3}, \tag{10}$$

$$a_c = \left(b_1 + b_2\,\mathrm{erfc}\left[\left(\frac{b_3}{Pr}\right)^{b_4}\right]^{b_5}\right)\tau_c^{-1/2}. \tag{11}$$

Corresponding values of the parameters a_j are given in Table 2. For higher values of the Prandtl number ($Pr > 1000$), $\tau_c = a_\infty Ra^{-2/3}$ and $a_c = b_\infty \tau_c^{-1/2}$ replace (10) and (11), respectively. Here, $a_\infty = 7.531$ and 4.207, $b_\infty = 0.533$ and 0.317, for the rigid–rigid and free–rigid cases, respectively.

Table 2
Parameters a_j and b_j of Eqs. (10) and (11) for the rigid–rigid (RR) and free–rigid (FR) conditions

j	a_j		b_j	
	RR	FR	RR	FR
1	9.8371	5.9017	0.5291	0.3066
2	1.9022	1.3279	0.2923	0.5002
3	2.0867	2.5505	0.6329	1.1196
4	0.8502	0.7730	0.3347	0.1971
5	1.1421	1.3132	2.0924	3.2267

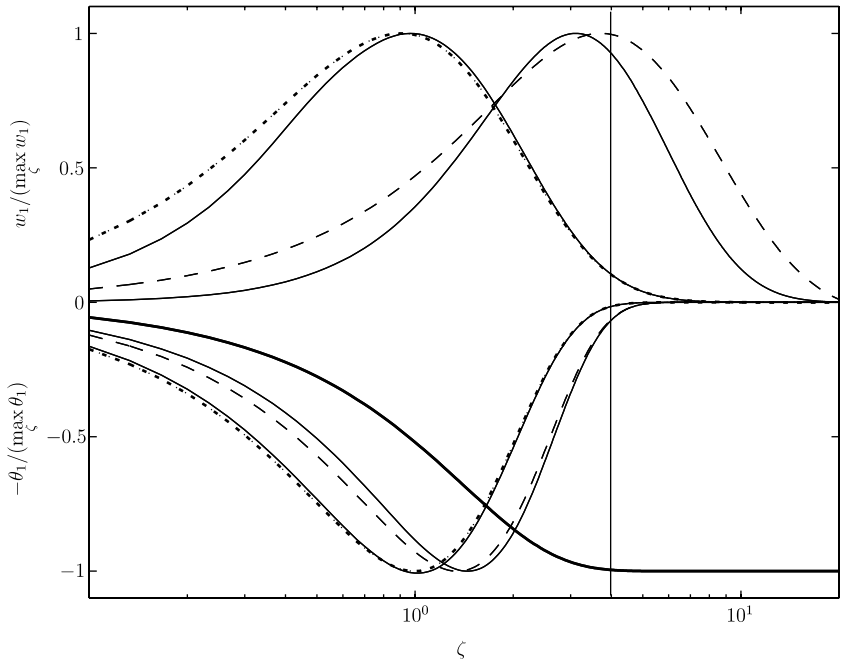

Fig. 3. Normalized amplitude functions for (minus) temperature and vertical velocity disturbances (lower and upper half, respectively). Solid lines represent the rigid–rigid case in both sets. From left to right, the latter curves show computed results for $Pr = 0.01$ and $Pr \to \infty$. The dotted and dashed curves represent the free–rigid case for $Pr = 0.01$ and $Pr \to \infty$, respectively. The bold monotonic curve exhibits (minus) the base state temperature, given by (8).

The amplitude functions corresponding to the results in Table 1 are represented in Fig. 3. Here, a TBL can be defined as the ζ value for which the base temperature reaches a value of 0.99. This limiting condition is depicted in Fig. 3 with a vertical line. With this definition, the latter figure shows a tendency of the amplitude curves to displace out of the TBL with increasing Prandtl number. The same trend was previously observed by Kang and Choi [14] in the DP system associated with the Bénard–Marangoni convection.

For Prandtl numbers greater than about one, it is found that vertical velocity disturbances reach depths that exceed by a factor close to 2 the thermal penetration depth. The increasing of the penetration of disturbances with Prandtl number means that the higher the latter parameter, the deeper is the layer where disturbances exist (Fig. 3). At the same time, as the Prandtl number increases, the system becomes less stable as shown by the monotonically decreasing marginal stability curves of the upper panel of Fig. 2.

An interesting feature of the eigenfunctions is that only for medium to large Prandtl numbers (greater that about 10) the asymptotic decay of the disturbances with depth in the case of the free–rigid case is noticeably slower than in the rigid–rigid case (Fig. 3). This trend is consistent with the separation between the stability curves for different boundary conditions depicted in Fig. 2 (upper panel), which appears to be minimum for low Prandtl numbers and maximum in the infinite Prandtl number case. As some liquid metals, like mercury, have very low Prandtl numbers ($\sim$0.025 at room temperature), present results suggest a way to avoid the kinematic effect of the boundary condition in laboratory experiments with a proper choice of the fluid.

Computed critical wavenumbers exhibit slight variations with the Prandtl number, for values of this parameter lower than about 0.1 and larger than about 10 (Fig. 2, lower panel). In the intermediate range ($0.1 < Pr < 10$), however, they present rather steep change rates with Pr. As the onset of convection is marked by the formation of regular cells, within the intermediate Pr range those disturbances should be rather more sensitive to small spatial variations in fluid properties than in the low and high Pr cases. Consequently, it is believed that this factor may influence to some extent the reproducibility of experiments and possibly explain in part the large dispersion in the horizontal wavelengths experimentally obtained by [8, Fig. 4].

Present results have some differences with respect to previous numerical calculations using other approaches to the stability analysis. In particular, in the amplification model [7] an amplification factor, built upon the normalized RMS of the disturbance of the vertical velocity field, is defined as $\bar{w}(t) = [\int_0^1 \tilde{w}_1^2(z,t)\mathrm{d}z / \int_0^1 \tilde{w}_1^2(z,0)\mathrm{d}z]^{1/2}$, where $\tilde{w}_1(z,0)$ represents the initial disturbance condition, which has been commonly chosen as white noise with equal amplitude coefficients (see [7,33,5]). When $\bar{w}(t)$ grows beyond some predefined factor, the corresponding time is marked as the onset time. In this context, different thresholds for $\bar{w}$ induce the estimation of different times. Such need for a definition of limiting conditions precludes a straightforward comparison between results coming from different

methods and care should be taken. The onset time predicted by the present method is analyzed in more detail next.

4.4. Analysis of onset time

To assess the onset time, commonly three classes of characteristic times are considered. The first corresponds to that which comes indirectly from the eigensystem (4), τ_c. The second one is that which marks the thermal dominance of advection over diffusion, τ_u. Finally, the third one is that at which fluid motion or temperature increase can be experimentally detected, τ_m. It is likely that the better the experiment, the closer is τ_m to τ_u since normally scalar change sensing is used. Experimental verification of τ_c seems to be more difficult, as it marks the beginning of convection, with a very small amplitude fluid motion [8,23,24,15,16]. On the other hand, there must be a lapse of time when velocities are small enough to make the advective term in the energy equation negligible compared with the diffusive one [34], that is $0 < w_1^* \tilde{\partial}_{z^*} \tilde{\theta} \ll \alpha \widetilde{\Delta} \tilde{\theta}$ for τ such that $\tau_c < \tau < \tau_u$. Then, τ_c must always be lower that τ_u.

In the case of results for the rigid–rigid case, Kim et al. [11] supported the conjecture of Foster [8] about the existence of a scaling factor of about 4, between time τ_c coming from eigenvalue calculations and time τ_m corresponding to observations of convective motion. To this purpose, they used the propagation model with the temperature step change setup and compared their theoretical results with the experimental ones by Ueda et al. [35]. Further comparisons were later reported by the same research group [27,16, and references therein] for large Prandtl numbers.

For the free–rigid case, theoretical results using the amplification model are given by Foster [7] for step and ramp changes in surface temperature with an isothermal bottom and some *Ra*–*Pr* combinations. However, no experimental results were available to validate the former case. Also in a theoretical framework, for $Pr = 7$ and free–free conditions, defining the onset time, τ_u, from a Nusselt number departure of 1% above the conductive state, Jhaveri and Homsy [9], found that $\tau_u \sim Ra^{-2/3}$ (named hereafter as the $-2/3$ power law), and also that $a_c \sim Ra^{1/3}$, showing that the latter relations hold for $Ra \geqslant 30 \times (27/4)\pi^4 \approx 2 \times 10^4$, which is close to the corresponding lower limit of this parameter proposed in Table 1. From their data and onset time definition (considered herein as being representative of τ_u), the value $Ra\tau_u^{3/2} \approx 350$ is obtained. This value is greater than the critical $Ra_\tau = 12.68 = Ra\tau_c^{3/2}$ obtained from Table 1, thus giving a value of the ratio $\tau_u/\tau_c = (350/12.68)^{2/3} \approx 9.1$.

In Fig. 4 (right panel), results from both the present propagation theory and the amplification model [7] for different Prandtl numbers and $Ra = 10^6$ are shown. It can be seen that for the free–rigid case both models differ on

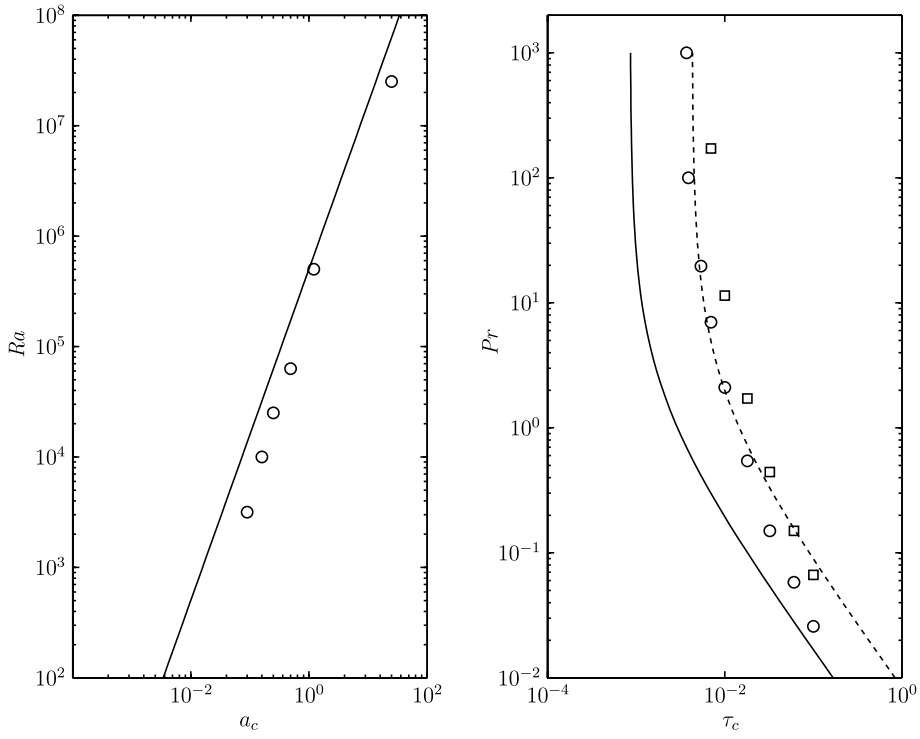

Fig. 4. Left panel: comparison between critical wavenumbers computed using the present propagation model (solid line) and the ones reported by Foster [7] (circles), for the free–rigid case, step change in temperature, with $Pr = 7$. Right panel: critical time as a function of Prandtl number; comparison between results obtained using propagation and amplification models with $Ra = 10^6$. Solid line represents results obtained with the present propagation model, while the dashed line shows the latter predictions amplified by a factor of 5. Circles represent results from Foster [7], using an amplification factor $\bar{w} = 10$; squares represent equivalent results with $\bar{w} = 100$.

computed onset times by a factor close to 5, when $\bar{w} = 10$ is used as an amplification factor, and the Prandtl number is greater than about 10. For lower values of Pr, the propagation model yields higher onset times than the ones found using the amplification model. It is noteworthy that the best amplification ratios for the rigid–rigid experiment by Foster [8] were found between $\bar{w} = 10^3$ and 10^8 (the latter theoretical calculations were previously reported by Foster [36]). Taking these results into account, it can be concluded that the tuned amplification factor can also be understood as a measure of the disturbance level that a system can afford just before the onset of convection. Wavenumbers were calculated with the present model using the data for $Pr = 7$ shown in Table 1, i.e., $a_\tau = 0.447 = a_c\sqrt{\tau_c}$. Fig. 4 (left panel) shows good agreement between present computations of the critical wavenumber a_c and those of Foster [7] for Rayleigh numbers higher than about 10^5, verifying the 1/3 power law scaling previously noted.

Experimental data for the free–rigid unsteady Rayleigh–Bénard case have been reported by Spangenberg and Rowland [17] and Foster [18], but a step in surface temperature was not obtained since evaporative cooling was the dominant effect. An approximate piecewise linear cooling on top was found experimentally. Using infrared radiometry to record surface layer temperature, the latter author compared his results with those obtained by the former, checking them against calculations made with the amplification model [7]. Good correspondence with this theory was found, however, due to the linear evolution of temperature on the top boundary, the experimental results fitted better a $-2/5$ exponent, instead of the $-2/3$ power law expected for the step change case. Table I of Foster [18] lists several results for the onset time given combinations of Prandtl and Rayleigh numbers. That table also includes results from Spangenberg and Rowland [17]. This data set agree well with amplification model calculations by Foster [7] using amplification factors between 10 and 100, showing that computed values of the onset times for low amplification and linear cooling describe well the onset of evaporative convection, as previously mentioned. On the other hand, the latter measurements yield times that differ in approximately three orders of magnitude with the present propagation theory results. Differences appear to reside solely on the different applicable power laws, with $\tau_{c\,\mathrm{step}}/\tau_{c\,\mathrm{linear}} \sim 10^{-3}$ in the range of Ra values analyzed, since for the step cooled system $Ra\tau_c^{3/2} = C_1$ (constant), while in the linearly cooled one the scaling is rather $Ra\tau_c^{5/2} = C_2$ (constant).

In the case of convection induced by gas absorption with free–rigid boundaries, defining a Rayleigh number based on a concentration step, $Ra = g\gamma(C - C_b)L^3D^{-1}\nu^{-1}$ (γ, C, C_b and D are the concentration coefficient of expansion, equilibrium and bulk concentration of solute and mass diffusion coefficient, respectively), along with the time scale L^2/D, Plevan and Quinn's data [19] yield measured dimensionless onset times $\tau_m \approx 2.1 \times 10^{-3}$ for carbon dioxide in water and $\tau_m \approx 1.3 \times 10^{-4}$ for sulphur dioxide in water. Although $Pr \approx 6.25$ in both cases, differences may come partly from the better solubility of the latter gas in water [20]. Corresponding time ratios, compared with that obtained from Eq. (10), are $\tau_m/\tau_c \approx 11$ and 13.1, respectively. Similarly, Blair and Quinn [20] found $Ra\tau_m^{3/2} \approx 300$ for sulphur dioxide in water. Using data from Table 1, time ratios are $\tau_m/\tau_c \approx 8.2$, 10.3 and 10.6, for Prandtl numbers of 7, 100, and 1000, respectively. In both works, $Ra \gtrsim 10^6$. Unfortunately, it is impossible to build similar relations with the experimental setup information from Tan and Thorpe [21], since no liquid layer thickness was specified in that paper. On the other hand, in the latter work, an alternative temporal and depth-dependent version of the Rayleigh number is proposed, along with a theoretical model where the solution of $Ra(z^*, t^*) = z^{*4}g\gamma\mu^{-1}D^{-1}\mathrm{d}C/\mathrm{d}z^*$ is maximized with respect to z^*, finding the length scale $L(t^*) = 2\sqrt{2Dt^*}$. The corresponding onset time is computed using the critical Rayleigh number in Bénard convection on a steady, horizontally infinite domain with free–rigid boundaries [37] on the expression for the maximum $Ra(z^*, t^*)$. From Tan and Thorpe [21] data, the latter was found to be on the order of 1000. Using $Ra(z^*, t^*)$ and $L(t^*)$ as the corresponding Rayleigh number and length scale, yields time ratios τ_m/τ_c close to 4, but their definitions are not analogous to the present Rayleigh number and length scale. Consequently, except for Tan and Thorpe's data [21], which provides no clue, all the revised references support the present estimation of a time ratio τ_m/τ_c on the order of 10, rather that 4, for the free–rigid system.

5. Concluding remarks

A stability analysis using propagation theory has been conducted to predict the factors that rule the temporal dependence of the onset of nonpenetrative convection in an initially isothermal Boussinesq fluid. It was shown that for the DP system, or, in other words, for high thermal disturbances, which are defined in terms of Rayleigh numbers that exceed a certain minimum for given Prandtl numbers (Table 1), the study of nonpenetrative convection equates conceptually and numerically the unsteady Rayleigh–Bénard convection. An extension of previously reported results for the rigid–rigid system using propagation theory [11] has been proposed for free–rigid boundary conditions. As several works have reported the study of the onset of unsteady Rayleigh–Bénard convection, a comparison of their results obtained with different methods, with those obtained using the present linear model was made. For Rayleigh and Prandtl numbers within the limits of the present theory, good agreement was found between present results and theoretical ones obtained with the amplification model [7] and the stochastic method [9]. General agreement on the validity of the scaling $\tau_c \sim Ra^{-2/3}$ was found. On the other hand, numerical evidence along with experimental data, suggest that the lag between theoretical onset times (τ_c) and detected ones (τ_u or τ_m) is dominated at least by

two conditions, namely, the kinematic boundary condition on the side where the heat flow (or temperature change) is imposed, and the way heating (or cooling) is applied in time. It is argued that, at difference from the theoretical determination of τ_c or τ_u, recording of τ_m depends in great extent on the experiment configuration and technological limitations. In particular, present results suggest that for medium to large Prandtl numbers (greater than about 1) and a top (if cooled from above) stress-free boundary, an onset time relation of $\tau_m/\tau_c \sim 10$ rather than 4 (previously proposed for the rigid–rigid system), seems to fit the available data reasonably well. Given these results, it is concluded that the latter values of the τ_m/τ_c ratio are particular cases of a more complex function that should take into account, at least, boundary conditions for the prediction of the onset of convective motion from the experimental knowledge of changes in scalar fields.

Acknowledgements

The authors gratefully acknowledge support from the Chilean National Commission for Scientific and Technological Research, CONICYT, the Department of Civil Engineering of the University of Chile, and Fondecyt Project No. 1040494.

References

[1] R.J. Adrian, Turbulent thermal convection in wide horizontal fluid layers, Exp. Fluids 4 (1986) 121.
[2] L. Rayleigh, On convection currents in a horizontal layer of fluid when the higher temperature in on the under side, Philos. Mag. 32 (1916) 529.
[3] R.B. Stull, An Introduction to Boundary Layer Meteorology, fifth ed., Kluwer Academic Publishers, 1988.
[4] P.G. Drazin, W.H. Reid, Hydrodynamic Stability, Cambridge University Press, 1981.
[5] P.M. Gresho, R.L. Sani, Stability of a fluid layer subjected to a step change in temperature: transient vs. frozen time analysis, Int. J. Heat Mass Transfer 14 (1971) 207–221.
[6] G.M. Homsy, Global stability of time-dependent flows: impulsively heated or cooled fluid layers, J. Fluid Mech. 60 (1973) 129.
[7] T.D. Foster, Stability of homogeneous fluid cooled from above, Phys. Fluids (8) (1965) 1249–1257.
[8] T.D. Foster, Onset of manifest convection in a layer of fluid with a time-dependent surface temperature, Phys. Fluids 12 (1969) 2482–2487.
[9] B.S. Jhaveri, G.M. Homsy, The onset of convection in fluid layers heated rapidly in a time-dependent manner, J. Fluid Mech. 114 (1982) 251–260.
[10] K.H. Kim, M.U. Kim, The onset of natural convection in a fluid layer suddenly heated from below, Int. J. Heat Mass Transfer 29 (1986) 193–201.
[11] M.C. Kim, K.H. Choi, C.K. Choi, The onset of thermal convection in an initially, stably stratified fluid layer, Int. J. Heat Mass Transfer 42 (1999) 4253–4258.
[12] C.K. Choi, J.D. Lee, S.T. Hwang, J.S. Yoo, The analysis of thermal instability and heat transfer prediction in a horizontal fluid layer heated from below, in: Proceedings of the International Conference on Fluid Mechanics, 1988, pp. 1193–1198.
[13] M.C. Kim, D.Y. Yoon, C.K. Choi, Buoyancy-driven convection in a horizontal fluid layer under uniform volumetric heat sources, Korean J. Chem. Eng. 13 (1996) 165–171.
[14] K.H. Kang, C.K. Choi, A theoretical analysis of the onset of surface-tension-driven convection in a horizontal liquid layer cooled suddenly from above, Phys. Fluids 9 (1997) 7–15.
[15] T.J. Chung, M.C. Kim, C.K. Choi, Temporal evolution of thermal instability in fluid layers isothermally heated from below, Korean J. Chem. Eng. 21 (2004) 41–47.
[16] C.K. Choi, J.H. Park, H.K. Park, H.J. Cho, T.J. Chung, M.C. Kim, Temporal evolution of thermal convection in an initially stably-stratified horizontal fluid layer, Int. J. Therm. Sci. 43 (2004) 817–823.
[17] W.G. Spangenberg, W.R. Rowland, Convective circulation in water induced by evaporative convection, Phys. Fluids 4 (1961) 743–750.
[18] T.D. Foster, Onset of convection in a layer of fluid cooled from above, Phys. Fluids 8 (1965) 1770–1773.
[19] R.E. Plevan, J.A. Quinn, The effect of monomolecular films on the rate of gas absorption into a quiescent liquid, AIChE J. 12 (5) (1966) 894–902.
[20] L.M. Blair, J.A. Quinn, Onset of cellular convection in a fluid layer with time-dependent density gradients, J. Fluid Mech. 36 (1969) 385–400.
[21] K.K. Tan, R.B. Thorpe, Gas diffusion into viscous and non-Newtonian liquids, Chem. Eng. Sci. 47 (13/14) (1992) 3565–3572.
[22] R.J. Goldstein, R.J. Volino, Onset and development of natural convection above a suddenly heated surface, J. Heat Transfer—Trans. ASME 117 (1995) 808.
[23] I.F. Davenport, C.J. King, The onset of natural convection from time-dependent profiles, Int. J. Heat Mass Transfer 17 (1974) 69–76.
[24] D.J. Yang, C.K. Choi, Onset of thermal convection in a horizontal fluid layer heated from below with time-dependent heat flux, Phys. Fluids 14 (2002) 930–937.
[25] C.K. Choi, J.H. Park, M.C. Kim, The onset of buoyancy-driven convection in a horizontal fluid layer subjected to evaporative cooling, Heat Mass Transfer 41 (2004) 155–162.
[26] C.K. Choi, J.H. Park, M.C. Kim, J.D. Lee, J.J. Kim, E.J. Davis, The onset of convective instability in a horizontal fluid layer subjected to a constant heat flux from below, Int. J. Heat Mass Transfer 47 (2004) 4377–4384.
[27] M.C. Kim, H.K. Park, C.K. Choi, Stability of an initially stably stratified fluid subjected to a step change in temperature, Theor. Comput. Fluid Dyn. 16 (2002) 49–57.
[28] C.F. Ihle, Y. Niño, Global stability of nonpenetrative convection, Phys. Fluids, to be submitted.
[29] E.M. Sparrow, R.J. Goldstein, V.K. Jonsson, Thermal instability in a horizontal fluid layer: effect of boundary conditions and non-linear temperature profile, J. Fluid Mech. 18 (1964) 513–528.
[30] J. Mizushima, Onset of convection in a finite two-dimensional box, J. Phys. Soc. Jpn. 64 (7) (1995) 2420–2432.
[31] K. Chen, M.M. Chen, C.W. Sohn, Thermal instability of two-dimensional stagnation-point boundary layers, J. Fluid Mech. 132 (1983) 49–63.
[32] J. Imberger, J.C. Patterson, Physical limnology, Adv. Appl. Mech. 27 (1990) 303–475.
[33] E.G. Mahler, R.S. Schechter, E.H. Wissler, Stability of a fluid layer with time-dependent density gradients, Phys. Fluids 11 (1968) 1901–1912.
[34] J.W. Elder, Temporal development of a model of high Rayleigh number convection, J. Fluid Mech. 35 (1969) 417–437.
[35] H. Ueda, S. Komori, S. Miyasaki, H. Ozoe, Time-dependent thermal convection in a stably stratified fluid layer heated from below, Phys. Fluids 27 (1984) 2617–2623.
[36] T.D. Foster, Effect of boundary conditions on the onset of convection, Phys. Fluids 11 (1968) 1257.
[37] S. Chandrasekhar, Hydrodynamic and Hydromagnetic Stability, first ed., Clarendon, Oxford, 1961.